Preprint
UCRL-JC-141036

Ignition scaling laws and their application to capsule design

M. C. Herrmann, M. Tabak, and J. D. Lindl

This article was submitted to
42nd Annual Meeting of the Division of Plasma Physics
Quebec City, Canada
October 23-27, 2000

October 20, 2000

U.S. Department of Energy

Lawrence
Livermore
National
Laboratory

Approved for public release; further dissemination unlimited

Ignition scaling laws and their application to capsule design

Mark C. Herrmann, Max Tabak, John D. Lindl

Box 808 L-018

Lawrence Livermore National Laboratory

Livermore, California 94550

(October 20, 2000)

Abstract

In this paper a two pronged approach is taken to investigating the energy required for ignition of inertial confinement fusion capsules. A series of one dimensional LASNEX[1] simulations is performed to create a database of barely ignited capsules that span the parameter regime of interest. This database is used to develop scaling laws for the ignition energy in terms of both the stagnated capsule parameters and the inflight capsule parameters, and explore the connection between these two parameter sets. The second part of this paper examines how much extra energy is required to overcome the effect of the inevitable surface imperfections that are amplified during the implosion process and can lead to capsule break up in flight or to mix of cold fuel into the hotspot, both of which can cause the capsule to fail to ignite. By means of an example, the optimization of a capsule with fixed adiabat, drive pressure, and absorbed energy is performed; the capsule that is maximally robust to these failure modes is found.

Typeset using REVTEX

I. INTRODUCTION

How much energy is needed to robustly ignite a given inertial confinement fusion capsule? This is of considerable interest in the optimization of an inertial fusion driver, since the energy the driver must supply is a monotone function of the energy required in the capsule. The yield of the capsule will typically exhibit a behavior like that shown in Figure 1, as the imploding fuel energy is increased the capsule yield increases slowly until the ignition energy is reached, after which the yield rapidly increases to some value and remains there. For the purposes of this paper, the ignition energy (E_{ign}) is defined as the fuel energy where the capsule gain (capsule yield over capsule absorbed energy) is 1. In the first part of this paper the dependency of (E_{ign}) on the various parameters of the capsule implosion will be examined by creating a database of barely ignited capsules and using this database to calculate a scaling law. Much of this work summarizes previous work by the authors[2] investigating the energy required for ignition, which in turn was prompted by discrepancies in computational scaling laws found by Levedahl and Lindl[3] and Basko and Johner[4].

In the absence of perturbations, a capsule would be designed with an energy just above E_{ign} so that the maximum capsule gain (Yield/capsule absorbed energy) would be achieved. However, in the presence of perturbations, the yield versus fuel energy typically shifts to higher energy as seen in Figure 1. Thus, in order to get the full gain, the capsule must be designed with some margin relative to the unperturbed ignition energy. However, for fixed driving pressure and energy budget there is a conflict betweeen increasing the implosion velocity (and 1D margin) and the increased hydrodynamic instability growth associated with it. In the second part of this paper the issue of how much margin is needed will be addressed by considering the optimization of high-yield capsule.

II. IGNITION SCALING LAW

A. Capsule Parameters

Before investigating the energy required for ignition it is useful to understand what independent variables matter for capsule implosions (and therefore can matter for the ignition energy).

After the shocks have passed through the capsule, and the peak drive power is reached, a typical capsule implosion approaches a state of an uniformly accelerating equilibrium as seen in Fig. 2. This state can be described by solving the hydrodynamic equations in the limit of a thin shell:

$$\rho g = -\nabla p, p\left(r_0\right) = P, p(r) = \alpha\rho^{5/3} \tag{2.1}$$

$$\rho(r) = \rho_{peak}\left(1 + \frac{2(r - r_0)}{5\Delta}\right)^{3/2} \quad r > r_0 - \frac{5}{2}\Delta \tag{2.2}$$

$$v(r) = \text{const}, \Delta \equiv \frac{m}{4\pi\rho_{peak}{r_0}^2} \tag{2.3}$$

where P is the applied pressure, $\rho_{peak} = (P/\alpha)^{3/5}$ and the fuel is assumed to be isentropic. The capsule will remain in this state until spherical effects (such as convergence or the back pressure of the fill gas) begin to matter. If only capsules with a fixed gas fill and implosions that are well tuned so that the fuel is nearly isentropic are considered the implosion can be characterized by 4 parameters: m, the fuel mass, P, the drive pressure, α_{if}, the inflight value of the adiabat (the ratio of the fuel pressure to the Fermi degenerate pressure) and v, the peak implosion velocity. These four quantities uniquely define a uniformly accelerating equilibrium which is the initial condition for the much more complicated physics of capsule stagnation, radiation and electron conduction losses and fusion burn that are involved in determining the capsule yield, so the yield of an ICF capsule can be thought of as a function of these four parameters. Note that capsules that have capsule gain 1 consist of a 3d hyperplane of this 4d implosion space.

Following Lindl, Chapter 5[5] these four parameters can be related to the capsule stability.

By energy conservation

$$PV \sim mv^2 \tag{2.4}$$

Take r_0 to be the radius where the peak drive begins, and Δr_0 to be the capsule shell thickness at this radius, then this can be written:

$$\frac{4\pi {r_0}^3}{3} P \sim 4\pi {r_0}^2 \Delta r_0 \rho v^2 \tag{2.5}$$

The ratio of the radius where peak drive begins to the shell thickness at that radius is :

$$\frac{r_0}{\Delta r_0} \equiv IFAR \sim v^2 \frac{\rho}{P} \sim \frac{v^2}{{c_s}^2} \equiv M^2 \tag{2.6}$$

$$IFAR \sim v^2 {\alpha_{\rm if}}^{3/5} P^{2/5} \tag{2.7}$$

where M is the Mach number, and the adiabatic relation has been used to write c_s in terms of $\alpha_{\rm if}$ and P. The in flight aspect ratio (IFAR) is a well known measure of capsule stability, the higher the IFAR the more unstable the capsule. Note that in deriving this relation mass ablation has been neglected (which is appropriate for direct drive, but inappropriate for indirect drive), however, even when significant mass ablation is present IFAR can be written in terms of v,$\alpha_{\rm if}$, and P (Lindl, Chapter 5[5]).

B. The isobaric model

After the imploding capsule converges sufficiently far the shell begins to stagnates on the gas at the center. The detailed profiles at this time become more complicated because, electron conduction, bremsstrahlung and fusion burn all become important in addition to the complicated hydrodynamics of a spherically converging compressible shell. However as the capsule stagnates it converts its kinetic energy into pressure, and goes from an implosion that is supersonic implosion to a stagnated state that is subsonic. As was understood by Meyer-ter-Vehn[6] this means that the pressure will be able to equilibrate and the capsule will become isobaric. Furthermore stagnated capsules typically have two distinct regions, a

high-temperature, low-density hot spot and a high-density, low-temperature cold fuel region. Taking the isobaric nature of the fuel, together with reasonable constraints on the hot spot in order for the capsule to ignite allows a simple model to be developed which can be used to estimate the energy required for ignition[6] in terms of the variables describing the stagnated state. Since the velocity of the imploding shell can be related to the hydrodynamic stability of the implosion[5], the minimum energy for "ignition" is expressed in terms of the implosion velocity. This leads to the well known scaling law for the ignition energy[7]:

$$E_{\text{ign}} \propto \frac{{\alpha_{stag}}^3}{{v_{\text{imp}}}^{10}} \tag{2.8}$$

where α_{stag} is the adiabat of the stagnated cold fuel.

C. Methodology

We must find a large number of marginally ignited capsules with values of m,v_{imp}, α_{if}, and P that span the range of interest for inertial confinement fusion. Tuning enough radiation driven capsules to get a meaningful database of marginally ignited capsules would be prohibitively time consuming. We choose to consider capsules that are composed of DT fuel only and are driven with a time varying pressure source applied on their outer surface. While care must still be taken to achieve a pulse that maintains the fuel as isentropic as possible, it turns out that this is much easier than tuning a radiation driven capsule.

The initial state of such a capsule is shown in Figure 3. Four parameters are used to specify a calculation: the mass of the fuel, m; the initial fuel aspect ratio, $\zeta = R_{in}/(R_{out} - R_{in})$; the strength of the initial shock, p_0; and the maximum drive pressure, P. These variables map onto four parameters, with the m and P being obvious, p_0 determines the capsule adiabat α_{if} and ζ and m can be used to determine the capsule volume which from Eq. 2.4 determines the implosion velocity. The DT gas fill is kept at 3×10^{-4}g/cm^3 for the capsules considered in this study.

To successfully implode these capsules, a pulse shape that goes from p_0 to P for a given m and ζ is needed. This pulse shape must be designed to keep the fuel as isentropic as possible.

If the inner fuel layers are not isentropic, the stagnation of the shell will be affected which, in turn, will cause the amount of energy required to ignite the capsule to change. The pulse shape chosen also must mimic, as much as possible, the drive which radiation driven capsules feel.

A generic pulse shape chosen to accomplish these goals is shown in Figure 4. The four shocks and ramp mimic the pressure at the ablator DT interface for typical radiation driven capsules. The four shocks are timed with an adaptive pulse shaper. The pulse shaper monitors the transit of the shocks through the capsule and the launching subsequent shocks so that the shocks do not overtake one another and that long rarefactions are avoided. The fuel remains quite isentropic. A typical entropy profile achieved by this pulse shaper is shown in Figure 5.

In accord with previous studies[3,4], a capsule is considered ignited if the fusion yield is eight times the work done on the capsule. (The factor of 8 accounts for the typical hydrodynamic efficiency of a radiation driven implosion which is about 12%.) To find the barely ignited capsules a one dimensional binary search over ζ (starting with initial values which give a subignited and superignited capsule) is performed. This typically takes between 10 and 20 LASNEX runs. Once a barely ignited capsule is found, the run is postprocessed to measure several variables of interest, which are then stored in a database of marginally ignited capsules.

To insure that these pressure-driven DT-only implosions do mimic radiation driven capsules, a radiation driven capsule has been compared with a pressure driven capsule with similar values of m,v,$\alpha_{\rm if}$, and P. As can be seen from Figure 6, which shows the density and pressure profiles of the two capsules at stagnation time, the stagnated states are quite similar.

Using the above prescription, marginally ignited capsules were found over a range of parameter space which encompasses what might be attempted on experiments in the foreseeable future (masses from 0.04 to 5 mg, p_0 from 1/2 to 8 MB, and P from 30 to 250 MB, which corresponds to marginally ignited capsules with $v_{\rm imp}$ from 2.0 to 5.0 10^7 cm/sec, $\alpha_{\rm if}$

from 0.6 to 3.0, and E_{ign} from 3.5 to 350 kJ).

D. Scaling Law using α_{stag}

Using the theoretical scaling law Eq. 2.8 as a model the database was fit to a power law of the form:

$$E_{\text{fit}}(\alpha_{\text{stag}}, v_{\text{imp}}) = C\frac{{\alpha_{\text{stag}}}^a}{{v_{\text{imp}}}^b} \tag{2.9}$$

Since the relative error is of more interest than the absolute error, the logarithm of Eq. 2.9 is taken and a linear least squares method is used to find the (a, b, C) which minimizes :

$$\sum_i \left(\log E^i_{\text{ign}} - a\log {\alpha_{\text{stag}}}^i + b\log {v_{\text{imp}}}^i - \log C\right)^2 \tag{2.10}$$

A best fit scaling law for the ignition energy was calculated using v_{imp} and α_{stag} as the variables yielding:

$$E_{\text{fit}}(\text{kJ}) = 2.1\ {\alpha_{\text{stag}}}^{2.66\pm0.06}\ \left(\frac{v}{3*10^7\text{cm/sec}}\right)^{-7.21\pm0.11} \tag{2.11}$$

This fit is quite good ($\sigma = 0.19$). A histogram showing the distribution of $E_{\text{ign}}/E_{\text{fit}}$ for the capsules in this study is shown in Figure 7.

E. Increase in the Adiabat During Stagnation

While the scaling law listed in Eq. 2.11 is useful, the adiabat at stagnation is not something which is directly under a capsule designer's control, unlike the four parameters listed in Section II A. Of course, if the capsule stagnation were adiabatic ($\alpha_{\text{stag}} \sim \alpha_{\text{if}}$), α_{if} could be substituted for α_{stag} in Eq. 2.11. To assess the degree to which stagnation is adiabatic the evolution of α was studied. Figure 8 shows a series of snapshots showing the evolution of the adiabat versus fuel mass, from the time of peak implosion velocity (lowest curve) to the time of stagnation (highest curve). Three important features are 1) a gradual increase in the value of α before stagnation which is due to DT not being exactly a $\gamma = 5/3$ gas, 2)

the gradual increase in adiabat which occurs for both the shocked and unshocked fuel after stagnation begins, and 3) the rapid change in adiabat versus fuel mass which is due to the stagnation shock propagating out through the fuel.

The first of these can be understood by examining the QEOS[8] equation of state for DT which was used in these calculations. Note that the pressure at the time of peak implosion velocity ranges from 30 to 500 MB for the capsules we are considering, whereas the pressure at stagnation time is in the 100's of GB. At very large pressures, DT approaches an ideal $\gamma = 5/3$ gas, however, in the pressure range where we are measuring $\alpha_{\rm if}$, it is still increasing with pressure.

The second effect mentioned above is due mainly to the deposition of energy from fusion neutrons created by the burning hot spot. While these neutrons are not coupling much energy to the fuel due to their long ranges, they do dominate over all sources other than the stagnation shock. Both α-particle deposition and electron conduction occur over too short a range to significantly affect fuel far from the hot spot. At typical hot spot temperatures near stagnation time (8 keV) the bremsstrahlung power is 6 times lower than the neutron power. Furthermore the energetic photons created by the bremsstrahlung (with energies on the order of the electron temperature) typically have ranges in deuterium-tritium plasmas longer than a 14 MeV neutron range.

The effect of the stagnation shock on the capsule adiabat can be studied in self-similar solutions for hollow spherical shells[9,10]. These analytical solutions behave in many ways like a stagnating ICF capsule. For shells coming in at high Mach number (as in ICF), the stagnation shock is launched when the shell hits the axis, this shock then propagates out from the center leaving an isobaric region of material which is essentially stopped behind it. The density and pressure versus radius at different times from such an implosion is shown in Figure 9, for a Mach number = 8.5 implosion. The stagnation shock starts at the axis at t=0 and propagates back through the fuel. Meyer-ter-Vehn *et al.*[9,10] found that for a $\gamma = 5/3$ gas, the pressure and density of a fluid element after the stagnation shock passed

can be related to the pressure and density of the same fluid element at t=0 :

$$P_f \sim P_0 M^3 \tag{2.12}$$

$$\rho_f \sim \rho_0 M^{3/2} \tag{2.13}$$

where M is the Mach number of the implosion. This implies:

$$\alpha_{stag} \sim \frac{P_f}{{\rho_f}^{5/3}} \sim \frac{P_0}{{\rho_0}^{5/3}} \sqrt{M} \tag{2.14}$$

$$\Rightarrow \alpha_{\text{stag}} \sim \alpha_{\text{if}} \sqrt{M} \sim {\alpha_{\text{if}}}^{0.85} v^{0.5} P^{-0.1} \tag{2.15}$$

where the sound speed is written in terms of the pressure, P, and the inflight adiabat, α_{if}, ($c_s \propto \sqrt{P/\rho}, \rho \propto P^{0.6}/{\alpha_{\text{if}}}^{0.6}$) when substituting for the Mach number. This suggests the adiabat increase during stagnation depends on the α_{if},v, and P.

In order to understand the combined effect of the three processes the database of marginally ignited capsules was fit to find the increase of the adiabat during stagnation. Following the example of Eq. 2.15 we fit α_{stag} using $\alpha_{\text{if}}, v_{\text{imp}}$, and P:

$$\alpha_{\text{stag}} = 3.2\ {\alpha_{\text{if}}}^{0.75\pm0.01} \left(\frac{v}{3 * 10^7 \text{cm/sec}}\right)^{0.44\pm0.03} \times \left(\frac{P}{100Mb}\right)^{-0.21\pm0.01} \tag{2.16}$$

which is not too different from the scaling law in Eq. 2.15.

To get a scaling law for the ignition energy in terms of parameters which the capsule designer can control Eq. 2.16 is substituted into Eq. 2.11 yielding

$$E_{\text{ign}} \sim {\alpha_{\text{if}}}^{2.00} {v_{\text{imp}}}^{-6.04} P^{-0.56}. \tag{2.17}$$

More generally the barely ignited database can be fit to a scaling law which includes the $\alpha_{\text{if}}, v_{\text{imp}}$, and P. This gives

$$E_{\text{fit } \alpha_{\text{if}}}(\text{kJ}) = 50.8\ {\alpha_{\text{if}}}^{1.88\pm0.05} \left(\frac{v}{3 * 10^7 \text{cm/sec}}\right)^{-5.89\pm0.12} \times \left(\frac{P}{100Mb}\right)^{-0.77\pm0.03} \tag{2.18}$$

which has a standard deviation similar to that of Eq. 2.11, (see Fig. 10). This scaling law is quite similar to Eq. 2.17, except for a slightly stronger inverse pressure dependence. Actually, if the drive pressure had been included as parameter in the fit with α_{stag} (Eq 2.11), there would have been a $P^{-0.22}$ dependence to the scaling law. Together with Eq. 2.17 this accounts for all of the pressure dependence in Eq. 2.18. While most of the effect of the pressure on the ignition energy comes by way of its effect on the increase in the adiabat during stagnation, some must arise from a change in the fuel configuration at stagnation time.

F. Comparisons to Radiation Driven Capsules

In order to ensure that the scaling law is valid it has been compared to radiation driven capsules and previous computational scaling laws. In Fig. 11 we compare the imploding fuel energy of a marginally ignited radiation, or directly driven capsule to the ignition energy predicted by the scaling law of Eq. 2.18 using the capsules' values of v, α_{if} and P. Over a large range of masses the scaling law does quite a good job of predicting the ignition energy. Note that the spread in the data is consistent with the spread in the data for the pressure driven capsules.

The generalized scaling law in Eq. 2.18 also explains discrepancies seen in previous computational studies[3,4] which were not understood. Levedahl and Lindl[3] and Basko and Johner[4] found that if the drive pressure is kept constant, as the implosion velocity and fuel adiabat of the capsule under consideration are varied, the minimum ignition energy scales like $E_{\text{ign}} \sim {\alpha_{\text{if}}}^{1.7}/{v_{\text{imp}}}^{5.5}$. In contrast, Basko and Johner found that when the pressure is varied in a hydrodynamically similar way which preserves the implosion Mach number ($P \sim {\alpha_{\text{if}}}^{-3/2}{v_{\text{imp}}}^{5}$), the ignition energy scales like $E_{\text{ign}} \sim {\alpha_{\text{if}}}^{3.0}/{v_{\text{imp}}}^{9.1}$.

Note that the dependence of E_{ign} in Eq. 2.18 on the pressure explains much of the

difference between these two results:

$$E_{\text{fit } \alpha_{\text{if}}} \sim \alpha^{1.9} v^{-5.9} \text{ for P constant} \tag{2.19}$$

$$E_{\text{fit } \alpha_{\text{if}}} \sim \alpha^{3.0} v^{-9.6} \text{ for P} \sim \alpha^{-3/2} v^{5} \tag{2.20}$$

G. Implications

The scaling law can be used to examined the tradeoff between energy, power, and stability. Solving Eq. 2.7 for v and substituting the result into Eq. 2.18 gives:

$$E_{ign} \sim \frac{{\alpha_{\text{if}}}^{1.8}}{v^6 P^{0.8}} \sim \frac{1}{IFAR^3 P^2} \tag{2.21}$$

Thus to lower the energy required for ignition IFAR or P must increase. In general, however, IFAR has some upper limit set by stability considerations and P has an upper limit set by the driver power intensity (or for the case of laser drivers, laser plasma interactions), and thus the minimum energy for ignition is set. The implications are shown graphically in Figure 12. Surprisingly the adiabat drops out implying, at least in the simplest case where only the IFAR determines the stability, there is no advantage to operating at high adiabat in order to achieve ignition. Of course these comments are true only in the limit where Eq. 2.7 is valid.

III. CAPSULE OPTIMIZATION

How can this scaling law for the ignition energy be used to aid in the design of capsules? For a given driver energy we may want to design the capsule with the maximum gain or we may want a capsule that is maximally robust to perturbations. In this section we will investigate, with the aid of the scaling law, how capsule perturbations affect the design of these two capsules.

In order to simplify this problem somewhat, consider the case where the adiabat and drive pressure are fixed. (It seems likely, given the Eq. 2.7 and Eq. 2.18 that both the

capsule gain and robustness will be maximized by operating at the highest pressure possible. Furthermore in the absence of perturbations the capsule gain and the capsule margin are maximized at the lowest possible adiabat. In the presence of perturbations, operating at the lowest adiabat may not maximize gain and performance[11] but we do not consider that case here). Furthermore, we assume the coupling efficiency of driver energy to fuel energy is nearly fixed so that the capsule fuel energy is also fixed.

A space of fuel energy versus velocity is shown in Figure 13. Contours of constant mass are shown in dashed lines. Since the adiabat and drive pressure are fixed the ignition energy from Eq. 2.18 is just a function of velocity, and in the absence of perturbations the space can be divided into a region of no ignition (below the red line) and ignition(above the red line). The green line shows a line of constant fuel energy. Thus the optimization question posed above becomes where on this line is the gain or the robustness maximized in the presence of perturbations. If there were no perturbations this question would be easy to answer. To maximize the gain, we want to implode the largest mass that ignites thus the capsule would operate very near where the ignition curve (red line) intersects the energy curve (green line). In contrast, for maximum robustness, we would want the maximum distance between the capsule and the ignition cliff, thus the capsule would operate at the maximum velocity possible.

The presence of perturbations changes both of these answers. For the case of maximum gain capsule imperfections grow during the implosion and can cause mix of cold fuel into the hot spot. This can delay ignition and, since the capsule is close to the 1 dimensional ignition cliff, can cause the capsule to fail. Thus capsules are typically designed with margin relative to the one dimensional ignition energy so that additional energy is available to ameliorate the effects of mix. For the case of maximum robustness, recall from Eq. 2.7 that the higher the implosion velocity the larger the IFAR, and therefore the more unstable the capsule is. If a capsule is very unstable, it may suffer from shell break up during the implosion and fail to ignite. Thus operation at too high an implosion velocity is unwise.

To summarize, where on the constant energy line do we want to design our capsules?

At the low velocity end capsules have high mass and therefore high yield. The perturbation growth is also low since low velocity corresponds to low IFAR from Eq. 2.7. However, the margin, relative to the ignition cliff is low. In contrast, at the high velocity end of the constant energy line, the yield is low (since the mass is low) and the perturbation growth is high (high v = high IFAR) however the margin is high.

For a concrete example consider an indirectly driven plastic ablator capsule which is of interest for heavy ion driven inertial confinement fusion because capsules with plastic ablator may be significantly easier to mass produce than the beryllium ablator capsules used in previous designs[12,13]. The capsule considered is shown in Figure 14. It has a nominal outer radius of 2.3 mm, absorbs approximately 900 kJ of energy and is driven with a pulse shape that has a foot temperature of 80 eV and a peak drive of around 265 eV.

To study the optimization consider four variants of this capsule, labeled Slow, Moderate, Fast, and Very Fast. The capsules are designed so that they have the same foot and peak drive and they absorb the same amount of energy to within 1%. The main difference is the amount of DT fuel mass each different variant has, as can be seen in Fig. 15. The position in energy-velocity space for the four capsules is shown in Fig. 16. The capsules do not lay precisely on the constant energy line due to variations in the hydrodynamic efficiencies of the implosions.

Several parameters for these capsules are shown in Table I. The margin is defined as the amount of fuel energy in the implosion divided by how much energy is required to ignite that capsule mass (graphically this is where the dashed lines in Fig. 16 intersects the 1D ignition cliff shown in red). These parameters follow the trends expected from above. The Slow capsule has high yield, low IFAR, and low margin, and the Very Fast capsule has nearly half the yield and twice the IFAR of the Slow capsule. However, it has significantly more margin.

The consequences of little margin can be seen in the behavior of the unperturbed capsules in Fig. 17. The central ion temperature is plotted parametrically versus the (ρr) of the hot spot for the four capsules. The capsules start cold and move towards higher temperatures,

while assembling their hot spot. Note that the blue curve (Slow capsule) reaches some maximum value of ρr and then its ρr starts to decrease before the capsule ignites. This corresponds to the capsule actually falling apart, and thus the capsule is igniting on the way out. In such circumstances a slight delay of ignition due to mix of hot spot into the cold fuel could prove disastrous, by giving the capsule a chance to fall completely apart before igniting. In contrast the very fast capsule (black curve) is still assembling its hot spot when it reaches ignition temperatures.

The consequences of high IFAR can be seen in Figure 18, which shows results from 2-D single mode growth factors for the four capsules versus Legendre mode number. These curves were created by seeding very small perturbations of the appropriate wavelength on the outside of the plastic at t=0. The implosion was then done and at the time of peak implosion velocity the size of the perturbation at the plastic-DT interface was measured and compared to the initial perturbation size in order to get a growth factor. As we move from Slow to very fast the peak of the spectrum moves out from 50 to 90. At the same time the growth factor increases by 6. This growth factor is a measure of how susceptible the various capsules are to shell break up, and thus suggests shell breakup may be a problem for the Very Fast capsule.

Another important indicator for capsules is the amount of growth that occurs at the hot spot-cold fuel interface near ignition time. This is significantly different from the growth at peak implosion velocity on the outside of the capsule, since the perturbations must feed through the shell and because these modes grow during the deceleration of the capsule. The net effect is to shift the growth to lower mode numbers. In Figure 19 the single mode growth factors at the hot spot interface at ignition time are plotted. While the very fast capsule does have the highest overall growth peaking above 2000 in mode 40, it is interesting to see that the slow capsule has higher growth rates than the moderate capsule for almost all the mode numbers and even has higher growth factors than the fast and very fast capsule for mode 15. This occurs because the slow capsule undergoes extra deceleration (and therefore extra deceleration growth) before it ignites; that is because it ignites on the way out, there

is more time for the deceleration growth to occur.

From these results it is impossible to determine which of the four capsules will be most robust. Thus we turn to multimode simulations, in which a spectrum of modes is seeded, with realistic amplitudes, on the outside of the ablator and on the inside of the DT ice layer, and then do 2D simulations on a 15° wedge of the perturbed capsule, resolving modes 12 to 160. These calculations were carried out in a way analogous to those done for NIF capsules[14,15] taking advantage of a novel tabular weighted opacity scheme developed by Marinak *et al.*[16].

It is currently not known what the spectrum or amplitude of surface or ice perturbations will be on capsules of this scale, indeed it is not entirely clear how to scale results from measurements of current capsule surface roughness to the capsule scale of interest. For simplicity we choose to study capsules with the same ablator roughness spectrum and ice roughness spectrum which has been used in the design of NIF ignition scale capsules[14,15]. To study the effect of increasing roughness we merely multiply the entire roughness spectrum by some number, thereby increasing the rms deviation of the surface from perfectly smooth. In Figure 20 a color coded density plot for the four capsules near the time of peak implosion velocity is shown. This simulation assumed 80 nm ablator roughness and 1 μm ice roughness. It is found that the ice roughness does not feed out significantly, and thus is not a big contributor to the perturbations that are seen for capsules of this scale. This is probably due to the fact these high-yield capsules are much thicker than ignition scale capsules. Note that the very fast capsule is perturbed significantly. The spike tips are at lower density than the rest of the fuel suggesting their entropy has been raised by radiation burning through the ablator. The bubbles are penetrating most of the way through the shell, suggesting that a rougher initial finish would have led to shell breakup. In contrast the slow capsule looks barely perturbed.

In Figure 21, density plots for the same capsules and same roughness are shown near ignition time. In contrast to the time of peak velocity all of the perturbations seem to be of comparable size in the four capsules at this time. There is a trend towards higher

mode number as we move from the slow capsule to the very fast capsule. Of course the single mode growth factors at ignition time (seen in Figure 19) show less variation between capsules than those at time of peak velocity which partly explains why the perturbation size scale is more similar. Another important effect is the nonlinear saturation of the instability, which becomes more important at small radii and at higher mode number[17]. Despite the perturbations seen here, all these capsules ignite and give a significant fraction of their clean yield.

A comparison of the capsule performance versus ablator roughness (with the ice roughness fixed at 1 μm) (Figure 22) provides the clearest indicator of the relative performance of each capsule. By examining the detailed simulations, we can conclude the slow capsule fails due to perturbations sticking into the hot spot delaying the ignition. In contrast, for the very fast capsule the shell breaks up from the outside and swirls material in again causing ignition to fail. Both the moderate and fast capsules, which have margin 1.3 - 1.6 have significant yield up to 200 nm initial ablator roughness, making them about twice as robust as the slow capsule and 1.6 times as robust as the very fast capsule. For reference the roughness associated with the NIF standard is shown in magenta, with an rms of 10-20nm. This specification is close to being met for plastic ignition scale capsules. Note that despite slow capsules poor performance relative to the moderate and fast capsule, for surface roughness below 80 nm or so it gives the maximum gain. As the initial surface roughness increases, the capsule which gives maximum gain and the capsule which is the most robust become one in the same until eventually ignition becomes impossible for the energy under consideration.

IV. DISCUSSION AND SUMMARY

In summary, we have developed a generalized scaling law (Eq. 2.18) for the ignition energy of ICF capsules which accounts for the effect of the drive pressure. We have found the plastic capsule which gives the maximum gain and the capsule that is maximally robust for a fixed absorbed energy , adiabat, and drive pressure. The answer depends on the

achievable surface finish. Future work will be to generalize the optimization to different absorbed energies, adiabats and drive pressures.

We have also done two dimensional stability calculations on high yield plastic ablator capsules which are of interest for inertial fusion energy and other high yield ICF applications. They appear to be significantly more robust than ignition scale targets, as they are able to withstand surface roughnesses from 10-20 times the NIF standard. This robustness might be used to relax the requirements for target fabrication, or capsules with higher IFAR (that require lower pressure) might be designed. These capsules would relax the driver power requirements.

ACKNOWLEDGMENTS

The authors would like acknowledge useful discussions with T. Dittrich, S. Haan, and M. Marinak. This work was performed under the auspices of the United States Department of Energy by the University of California Lawrence Livermore National Laboratory under contract No. W-7405-Eng-48.

REFERENCES

[1] G. B. Zimmerman and W. L. Kruer, Plasma Phys. Controlled Fusion **2**, 51 (1975).

[2] M. C. Herrmann, M. Tabak, and J. D. Lindl, Nucl. Fusion (2001), to be published.

[3] W. K. Levedahl and J. D. Lindl, Nucl. Fusion **37**, 165 (1997).

[4] M. M. Basko and J. Johner, Nucl. Fusion **38**, 1779 (1998).

[5] J. D. Lindl, *Inertial Confinement Fusion: The Quest for Ignition and Energy Gain Using Indirect Drive* (Springer-Verlag, New York, 1998).

[6] J. Meyer-ter-Vehn, Nucl. Fusion **22**, 561 (1982).

[7] M. D. Rosen, J. D. Lindl, and A. R. Thiessen, *Laser Programs Annual Report - 1983* (Lawrence Livermore National Laboratory, Livermore, CA, 1984), Chap. 3, pp. 5–9.

[8] R. M. More, K. H. Warren, D. A. Young, and G. B. Zimmerman, Phys. Fluids **31**, 3059 (1988).

[9] J. Meyer-ter-Vehn and C. Schalk, Z. Naturforsch. **37a**, 955 (1982).

[10] J. Meyer-ter-Vehn, in *Proceedings of the 29th Scottish Universities Summer School in Physics: Laser-Plasma Interactions: 3*, edited by M. B. Hooper (SUSSP Publications and Institute of Physics Publishing, London, 1985), Vol. 14, pp. 234–245.

[11] M. Tabak, D.H.Munro, and J.D.Lindl, Phys. Fluids B **25**, 1007 (1990).

[12] M. Tabak and D. A. Callahan-Miller, Phys. Plasmas **5**, 1895 (1998).

[13] D. A. Callahan-Miller and M. Tabak, Nucl. Fusion **39**, 1547 (1999).

[14] T. R. Dittrich *et al.*, Phys. Plasmas **5**, 3708 (1998).

[15] T. R. Dittrich *et al.*, Phys. Plasmas **6**, 2164 (1999).

[16] see National Technical Information Service Document DE-96004569 [M.M.Marinak,

R.E.Tipton, B.A.Remington, S.W.Haan, S.V.Weber, in ICF Quarterly Report(1995), UCRL-LR-105821-95-3]. Copies may be ordered from National Technical Information Service, Springfield, VA 22161. (unpublished).

[17] S. Haan, Phys. Rev. A **39**, 5812 (1989).

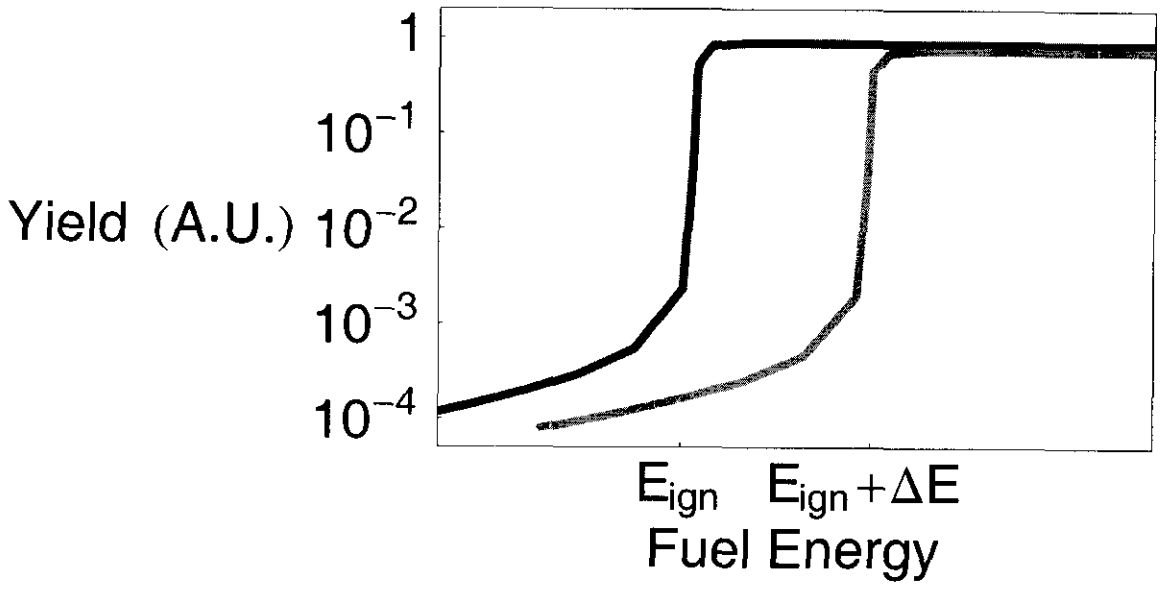

FIG. 1. Yield (A.U.) versus energy in imploding fuel for typical capsule.

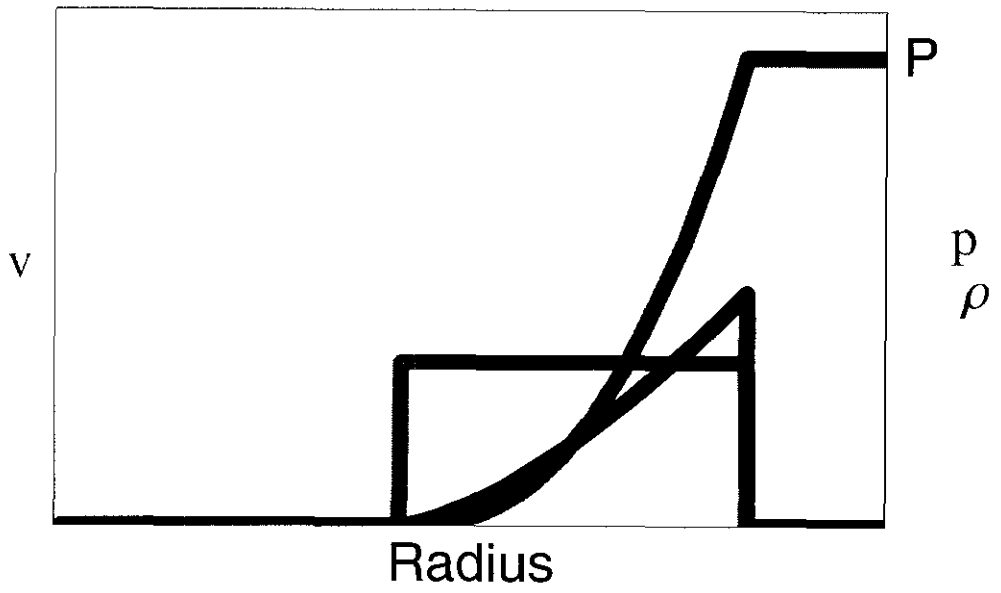

FIG. 2. Density, pressure, and velocity for a uniformly accelerating equilibrium.

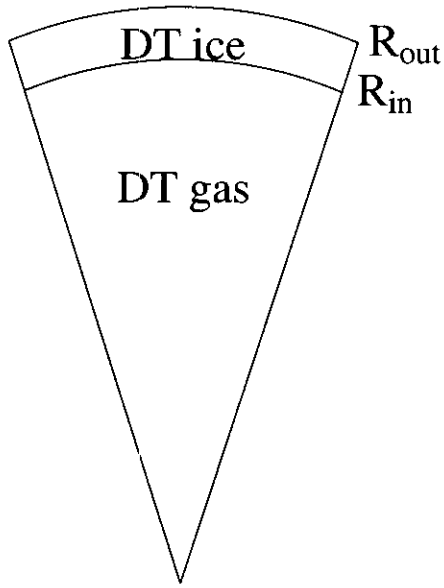

FIG. 3. Generic structure of capsules used in this study.

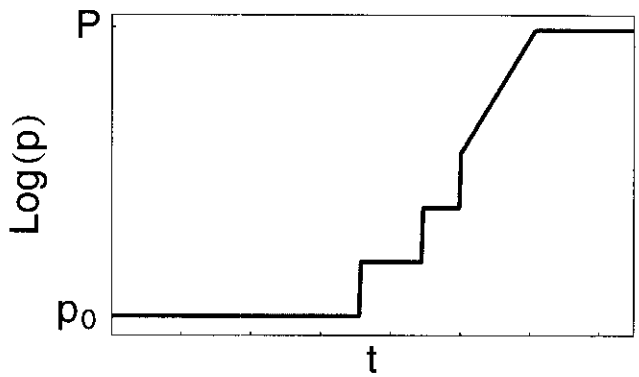

FIG. 4. Generic form of pressure pulse shape used to drive fuel only capsules.

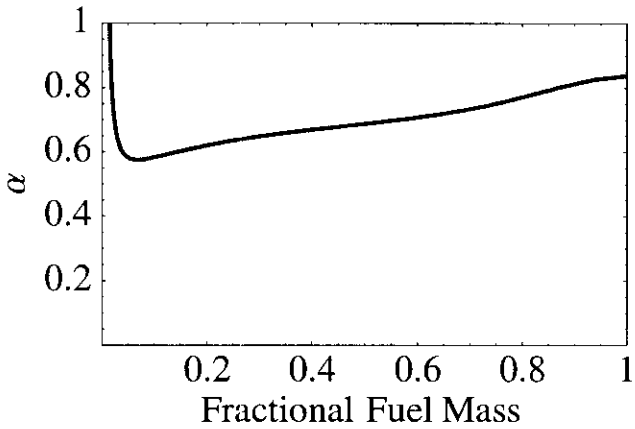

FIG. 5. Adiabat profile vs. fuel mass at peak implosion velocity.

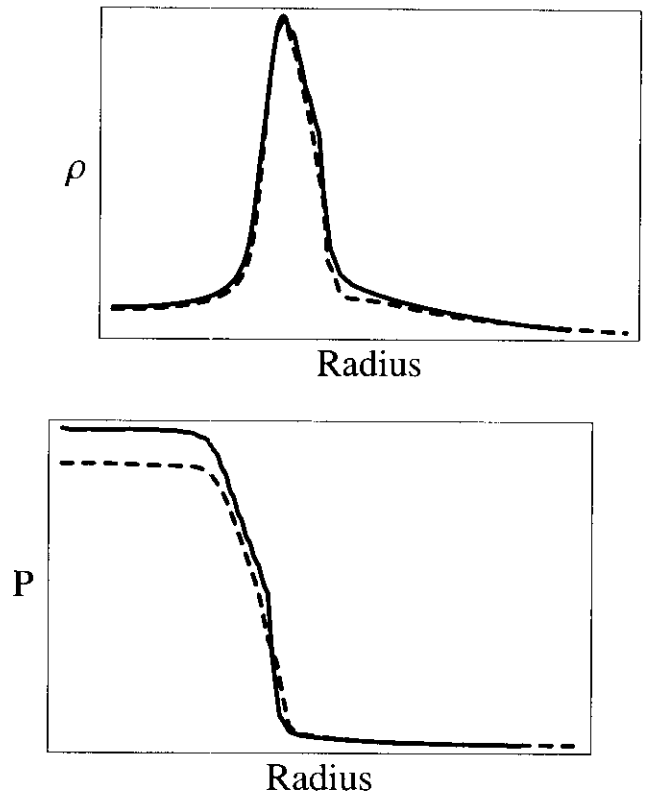

FIG. 6. A comparison of the stagnated states (at time of peak ρr) of two marginally ignited capsules, one pressure driven and one radiation driven, with similar masses, entropy profiles, peak pressures, and implosion velocities.

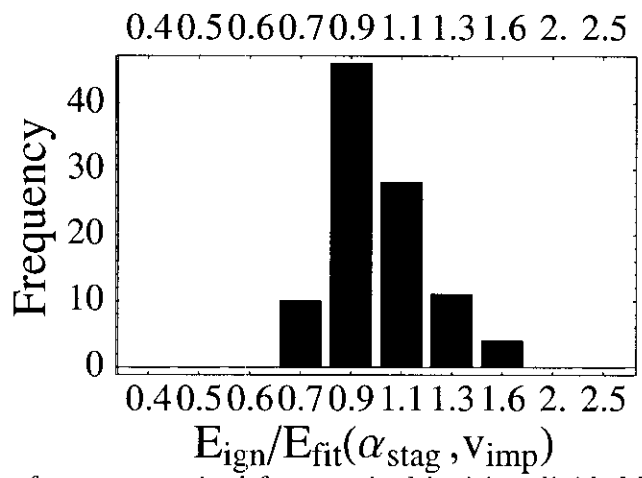

FIG. 7. Distribution of energy required for marginal ignition divided by the energy predicted by Equation 2.11 for the pressure driven capsules used in this study.

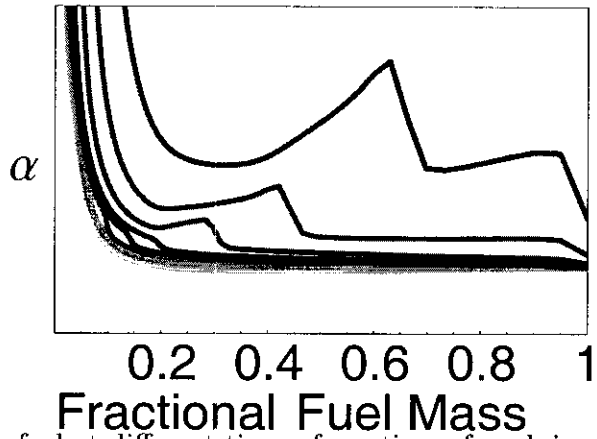

FIG. 8. Adiabat of the fuel at different times, from time of peak implosion velocity to time of stagnation.

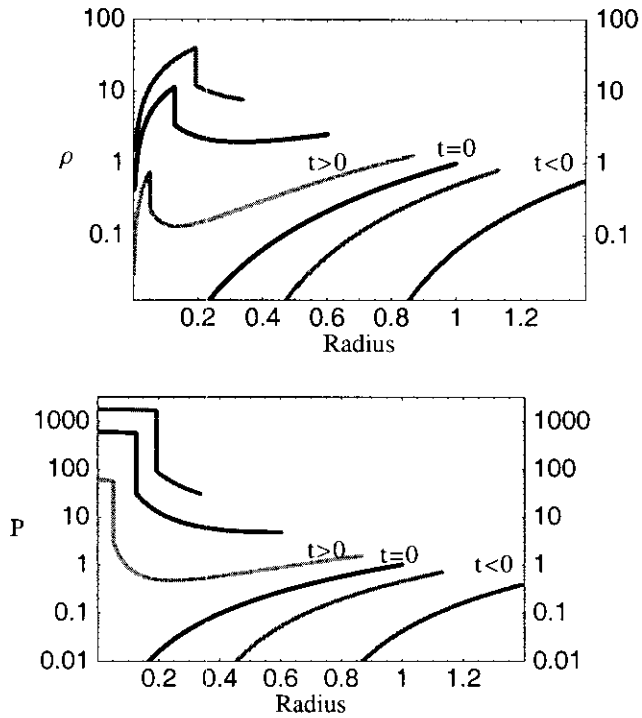

FIG. 9. Results from self-similar hollow shell implosions for Mach number 8.5 implosion, $\gamma = 5/3$

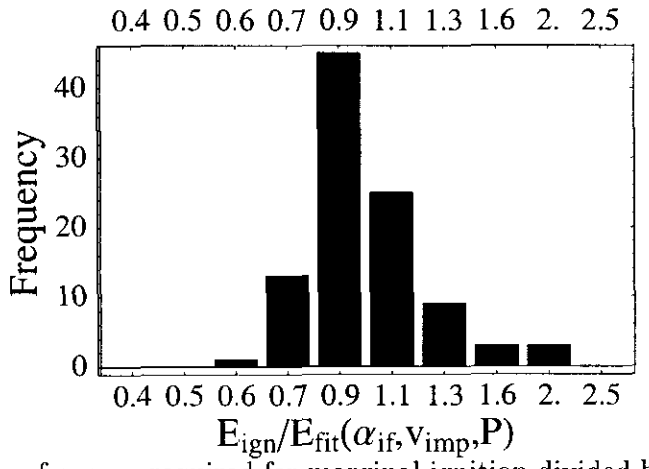

FIG. 10. Distribution of energy required for marginal ignition divided by the energy predicted by Equation 2.18 for the pressure driven capsules used in this study.

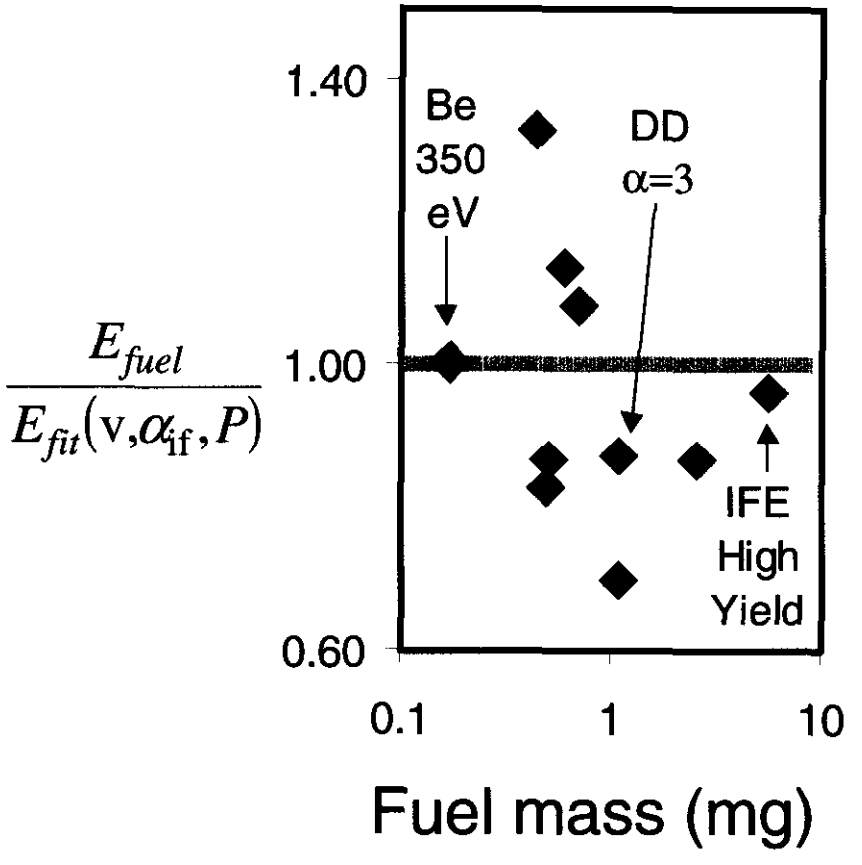

FIG. 11 Ratio of fuel energy for marginally ignited radiation and directly driven capsules to fit prediction from Eq. 2.18 using the capsules v, α_{if} and P plotted versus fuel mass.

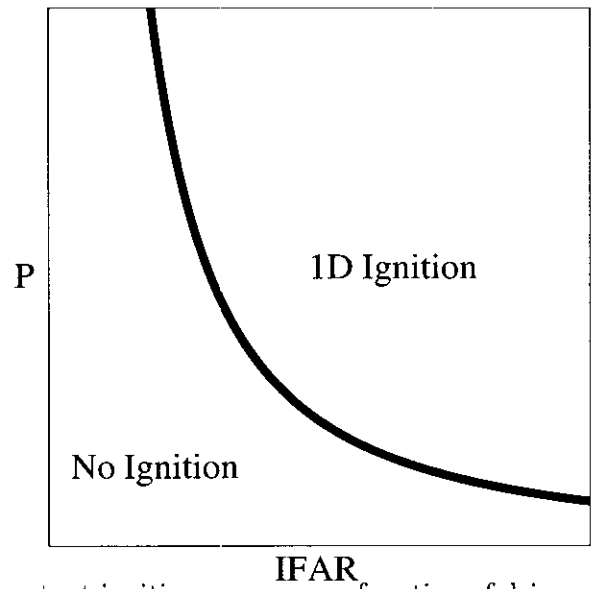

FIG. 12. Contour of constant ignition energy as a function of drive pressure and inflight aspect ratio. Note that the line delineates the space where ignition is possible and where it is not for a given energy.

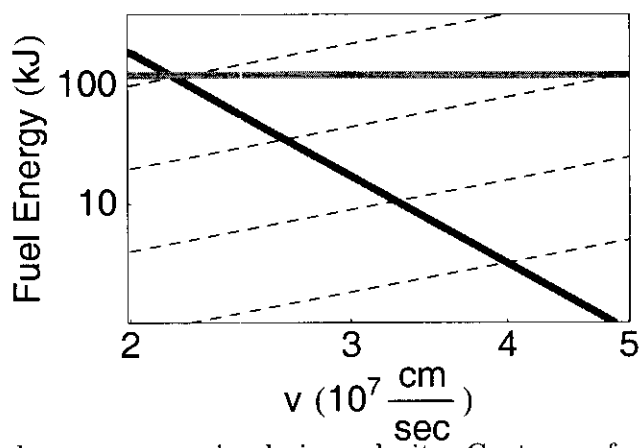

FIG. 13. Space of fuel energy versus implosion velocity. Contours of constant mass are shown in black. The red line shows the ignition energy for a fixed adiabat and drive pressure, the green line shows a line of constant energy.

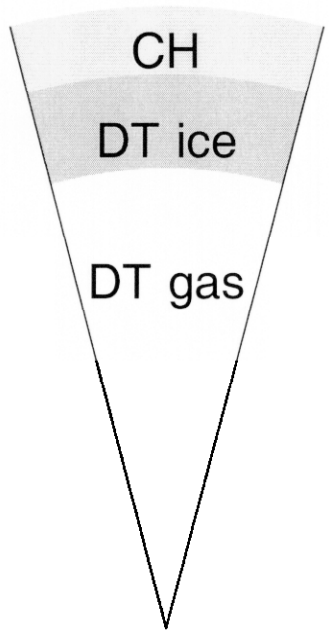

FIG. 14. The radial build of the capsule being optimized.

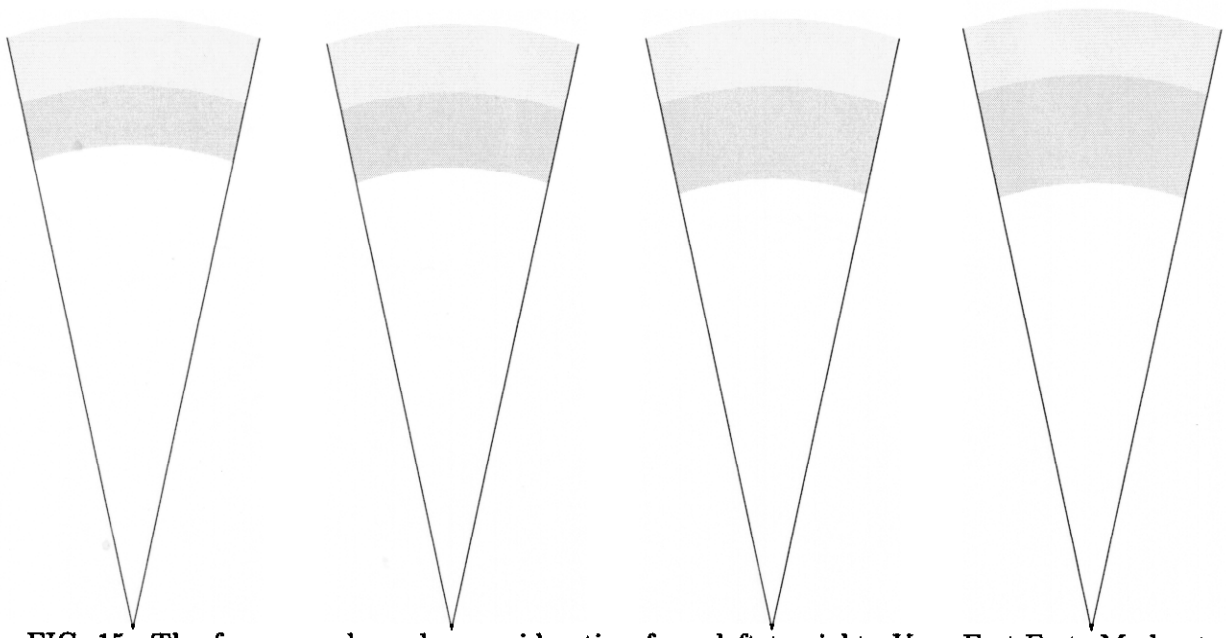

FIG. 15. The four capsule under consideration from left to right: Very Fast,Fast, Moderate, Slow.

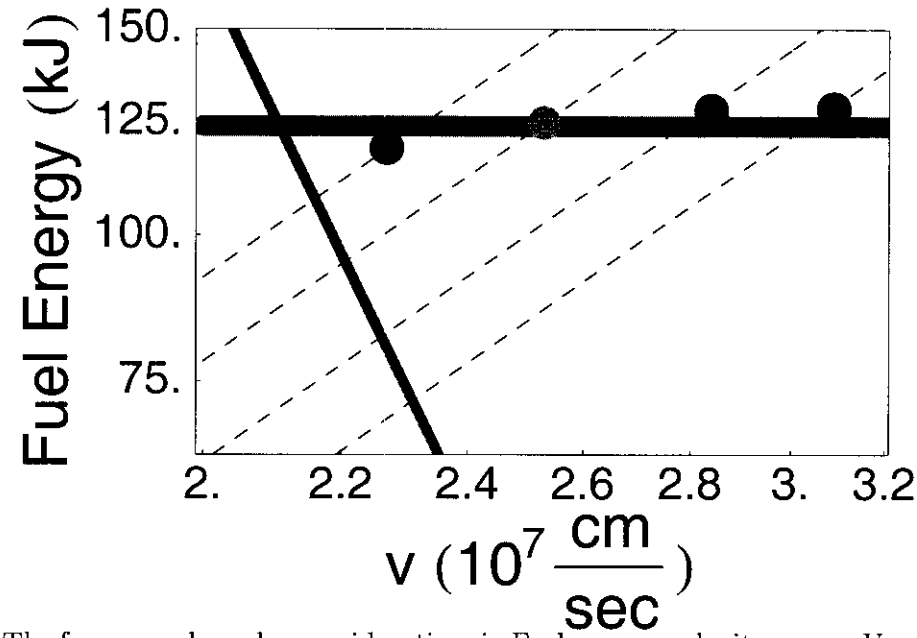

FIG. 16. The four capsule under consideration, in Fuel energy, velocity space. Very Fast (black), Fast (red), Moderate (green), Slow (blue).

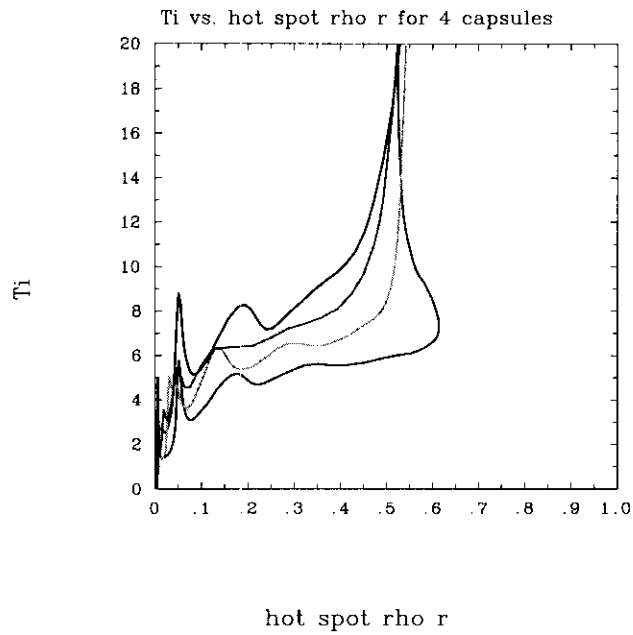

FIG. 17. Central T_i vs. ρr of the hot spot for four capsules Very Fast(black) ,Fast (red) , Moderate (green), Slow (blue).

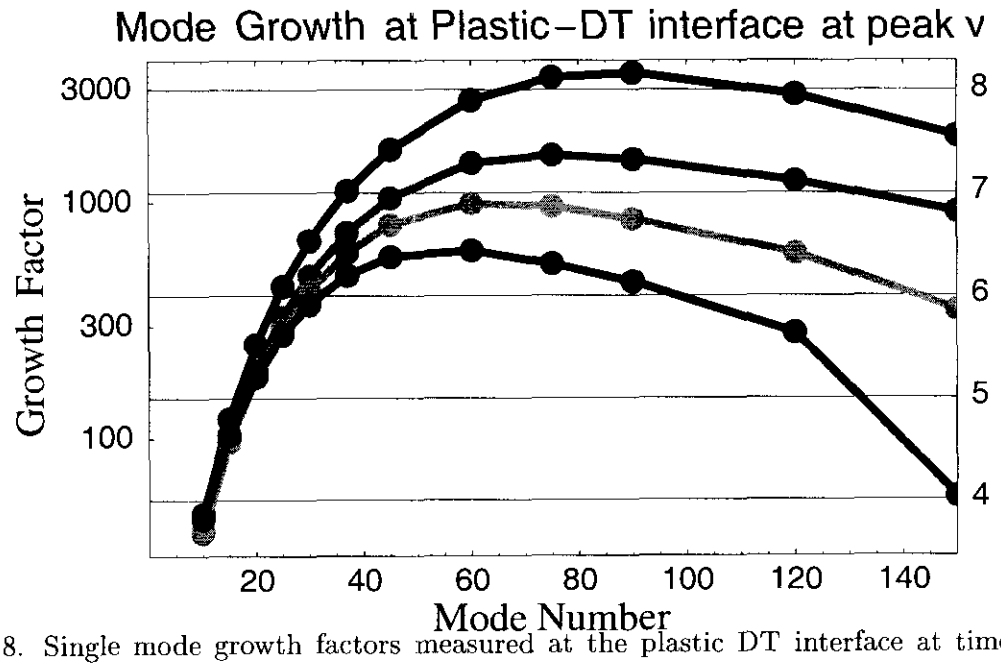

FIG. 18. Single mode growth factors measured at the plastic DT interface at time of peak velocity for the four capsules. Very Fast(black) ,Fast (red) , Moderate (green), Slow (blue).

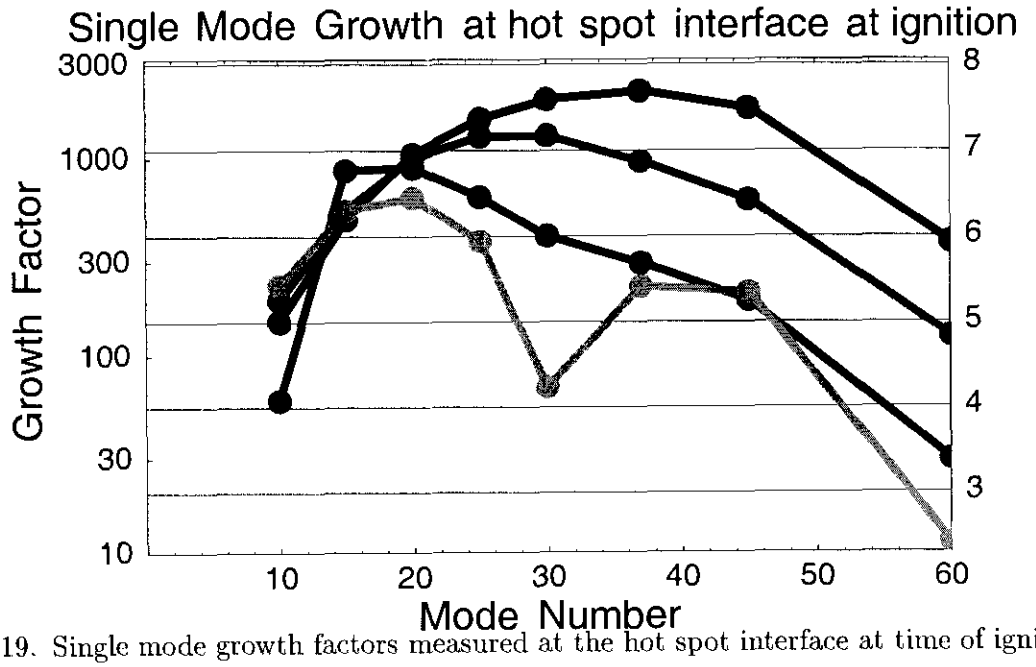

FIG. 19. Single mode growth factors measured at the hot spot interface at time of ignition for the four capsules. Very Fast(black) ,Fast (red) , Moderate (green), Slow (blue).

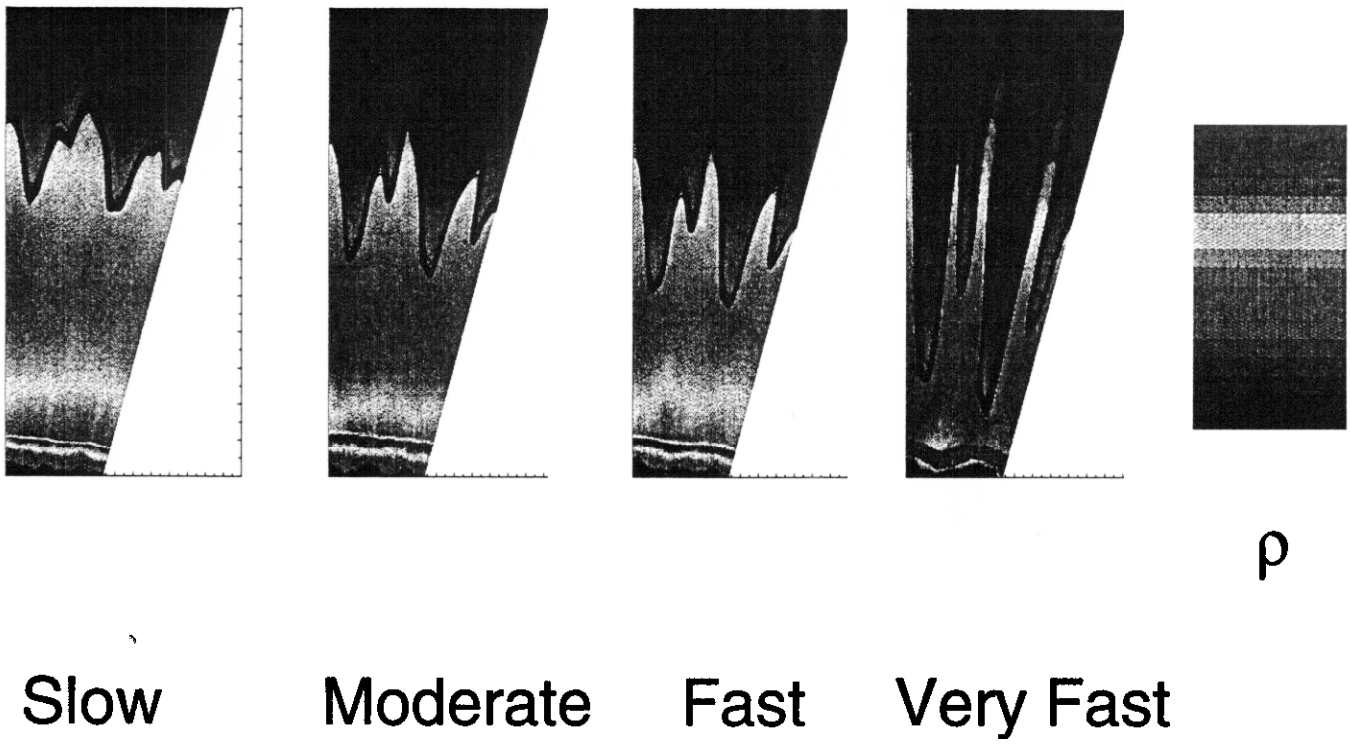

FIG. 20 Density from multimode simulations with initial surface roughness of 80 nm on the ablator and 1 μm roughness on the DT ice near time of peak velocity for the four capsules.

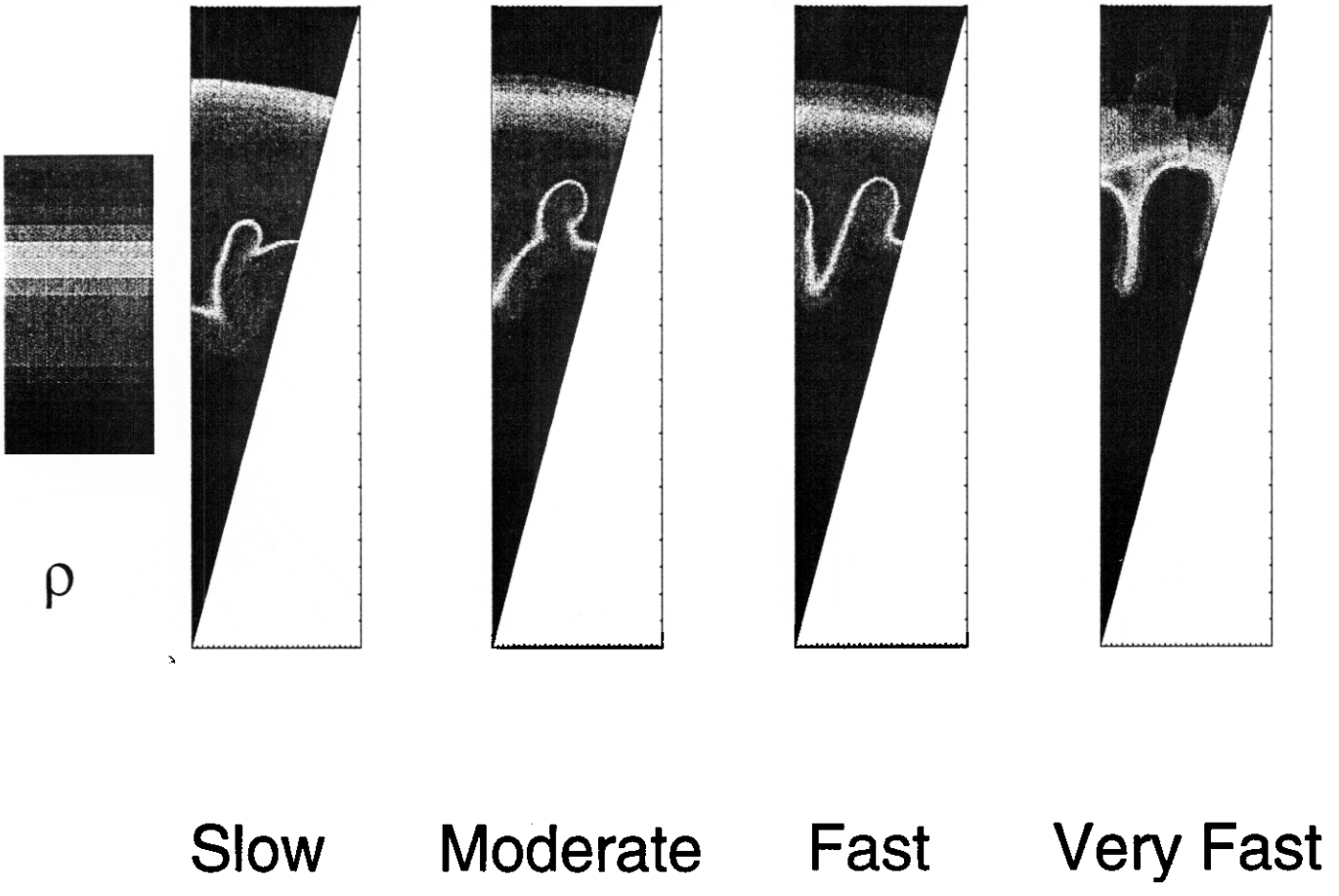

FIG. 21 Density from multimode simulations with initial surface roughness of 80 nm on the ablator and 1 μm roughness on the DT ice near ignition time for the four capsules.

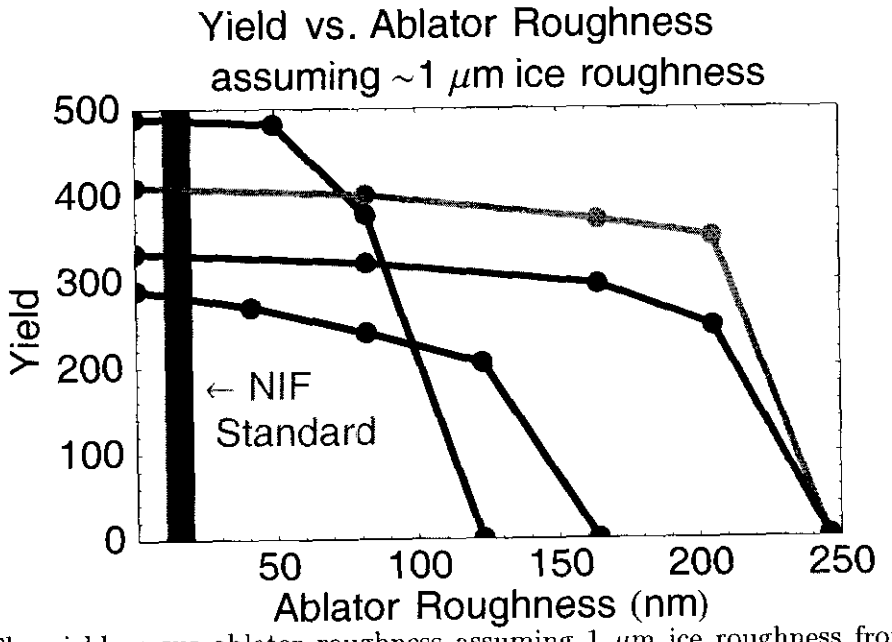

FIG. 22. The yield versus ablator roughness assuming 1 μm ice roughness from multimode simulations for the four capsules. Very Fast(black) ,Fast (red) , Moderate (green), Slow (blue).

TABLES

TABLE I. Parameters for the four indirectly driven capsules.

Capsule	Very Fast	Fast	Moderate	Slow
Mass of fuel (mg)	2.7	3.2	3.9	4.6
v_{imp-mw} $(10^7 cm/sec)$	3.1	2.8	2.5	2.3
Yield (MJ)	286	333	412	496
IFAR	50	45	38	26
Fuel Energy/E_{ign}	1.8	1.6	1.3	1.1